Applied Magnetic Resonance (2022) 53:1331–1343
https://doi.org/10.1007/s00723-022-01469-9

Applied
Magnetic Resonance

ORIGINAL PAPER

Methionine-Based Radicals: Time Scales and Species

Dmytro Neshchadin[1] · Anne-Marie Kelterer[1] · Chantal Houée-Levin[2] · Eduard Stadler[1] · Martin Spichty[3] · Georg Gescheidt[1]

Received: 14 June 2021 / Revised: 10 February 2022 / Accepted: 6 March 2022 /
Published online: 7 May 2022

Abstract

L-Methionine is an amino acid, which provides anti-oxidative properties. We report on radicals and radical cations being likely (short-lived) intermediates formed upon photo-oxidation reactions of methionine. In this context, we present photo-CIDNP experiments indicating that the character of the photooxidants is decisive for the observation of CIDNP effects based on methionine. Based on calculated hyperfine data and pK_a values and on our experimental observations, we suggest that CIDNP polarizations are produced by an overlay of at least three geminal radical pairs, i.e., two α-thio carbon-centered radicals **D**· and **G**·, aminyl radical **N**·, and, possibly, 2c–3e radical cation $\mathbf{SN}^{\cdot+}$ as short-lived reaction intermediates.

1 Introduction

L-Methionine (**1**) is an important natural antioxidant and a component in many proteins. The antioxidant effect of **1** is based on its primary (one-electron) oxidation and the subsequent formation of methionine sulfoxide, which, then is converted back to parent **1** by sulfoxide reductases [1]. The primary oxidation of **1** to its radical cation, $\mathbf{1}^{\cdot+}$, is rather subtle, because it has been shown to be electrochemically irreversible, depending on the pH value, and the material of the working electrode [2–4]. Accordingly, $\mathbf{1}^{\cdot+}$, must be regarded as highly reactive and very short-lived (at the time scale of electrochemical experiments). Beside the formation of sulfoxides,

This manuscript is dedicated to Kev Shalikhov and Klaus Möbius, still among the youngest scientists I know. Thank you, Kev and Klaus, for your friendship, dedication, and your critical eye.

✉ Georg Gescheidt
g.gescheidt-demner@tugraz.at

[1] Institute of Physical and Theoretical Chemistry, Graz University of Technology, Stremayrgasse 9/Z2, 8010 Graz, Austria

[2] Laboratoire de Chimie Physique, UMR 8000, Université Paris Sud, 91405 Orsay, France

[3] Laboratoire d'Innovation Moléculaire et Applications, 3 bis, rue Alfred Werner, 68093 Mulhouse, France

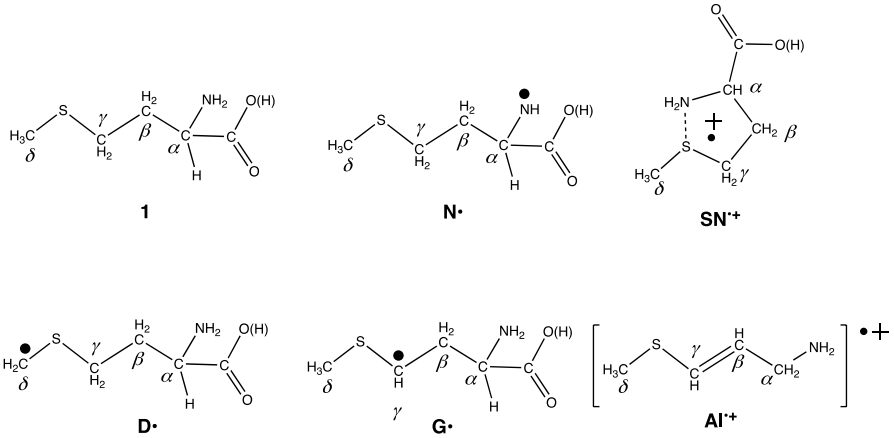

Scheme 1 Radicals based on **1** discussed in this manuscript (differently charged protonated, deprotonated, zwitterionic forms are omitted for clarity, accordingly, we have placed the hydrogen at the carboxyl group in brackets)

decarboxylation has been shown as an additional rapid decomposition pathway of $\mathbf{1}^{\cdot+}$; moreover, products with C=C double bonds adjacent to the thiol group have been found [5–7].

Accordingly, methods providing a faster time scale (ns–ms) have been utilized to obtain insights into the corresponding short-lived intermediates. Transient optical spectroscopy combined with deconvolution procedures of the absorption bands has been the method of choice to observe such species upon oxidation induced by pulse radiolysis [8–12]. These investigations point to the formation of radical cations derived from specific isomers based on $\mathbf{1}^{\cdot+}$ including two-center three-electron ((2c–3e) isomers, e.g., >S.·.S← bonded dimers ($\mathbf{2S}^{\cdot+}$, $\lambda_{max}=480$ nm), and intramolecular 6- and 5-membered rings with S.·.O–, ($\mathbf{SO}^{\cdot+}$, $\lambda_{max}=395$ nm) or >S.·.N– ($\mathbf{SN}^{\cdot+}$, $\lambda_{max}=390$ nm) bonding (Scheme 1) [8, 11, 13–23].

Magnetic-resonance spectroscopy was utilized to obtain additional insight into such intermediates. When matrices containing methionine were γ-irradiated, EPR spectra revealed [24, 25] the formation of radical cations based on $\mathbf{1}^{\cdot+}$, particularly indicating a species with an remarkably high isotropic ^{14}N hyperfine coupling constant (hfc) of ca. 3.3 mT [calculated from the anisotropic data in reference [24] upon γ-irradiation in LiCl and LiBr (150 K)] assigned to $\mathbf{SN}^{\cdot+}$. Already in 1973/83, Davies, Gilbert, and Norman have reported on the photooxidation of **1** in the presence of a Ti(III) salt dissolved in H_2O_2 [26, 27] in a flow system. They have assigned the hyperfine data to (deprotonated) methionine-based radicals **D**· and **G**· [2] (see also Table 1). These EPR findings were either based on radicals trapped in matrices at low temperatures or on the use of a fluid-solution system with a millisecond detection time scale. Chemically Induced Dynamic Electron Polarization (CIDEP) coupled to photo-induced reactions provides a substantially shorter time scale to detect hyperfine data of short-lived radicals. In the presence of sodium anthraquinone-3-sulfonate, **1** was photo-oxidized and the corresponding EPR spectra were

Table 1 Experimental (based on EPR, CIDEP, and CIDNP) and calculated (B3LYP/6-31G(d)) hfcs for various methionine-derived radicals and radical cations (for labeling, see Scheme 1)

Species	hfcs/mT							
	exp/calc	α	β	γ	$\delta(CH_3)$	^{14}N	$NH_{(2)}$	Ref.
N·	exp					1.34	2.19	[28]
N·	calc					1.46	2.20	This work
SN·$^+$	exp	0.14	0.0	0.74	0.83	0.01	0.96	[28]
	exp	0.87	–	0.78	0.72			[32][a]
		Big	Small	Big	Big			[29, 30][b]
	exp					3.3		[24][c]
SN·$^+$	calc	*2.88*	*0.13*	*0.64*	*0.73*	*2.42*	*1.05*	This work
AL·$^+$	calc	*0.03*	*0.57*	*0.28*	*0.68*	*0.43*	*0.85*	This work
D·	exp	–	–	0.21	1.64	–		[26]
D·	calc	*0.00*	*0.01*	*0.34*	*1.73*	0.00		This work
G·	exp	–	2.98[d]	1.68	0.29	–		[26]
G·	calc	0.00	*2.50* [d]	*1.93*	*0.24*	0.00		This work

The data taken from literature were limited to two-digit accuracy. (for clarity, the calculated values are represented in italics)

[a]Determined by time-resolved CIDNP for the 2c-3e methionine moiety in a Met–Gly dipeptide

[b]The authors of this contribution do not provide numbers or clear ratios but indicate positions with substantial hyperfine coupling constants for the α, β, and γ protons claiming that "Taking the dimeric radical cation of tetrahydrothiophene (a (H^a) = 0.93 mT [14]; this value must be doubled to describe a radical cation in which unpaired electron is located on a single sulfur atom) and the radical cation of *N*-methylpyrrolidine (average of the splittings the methylene a protons 4.25 mT) [15] as model compounds, one obtains that in the species Met-(S.·.N·$^+$) with the two-center three-electron bond about one third of the unpaired spin density is shifted from sulfur to nitrogen (r_S:r_N = 0.64:0.36). This statement, however, is misleading since the dimer mentioned does not comprise the rehybridization of the radical centers, which, however, is crucial in the case of 2c-3-bonding (see the corresponding references in the introduction)."

[c]According to the highly anisotropic and broad EPR signal, the authors can only provide data with rather high error margins. Nevertheless, their data basically correspond with the calculated values

[d]The original publication reports on a sum of 2.98 mT as a sum for the two protons in β position [26]. We have accordingly used the corresponding sum of the calculated values (2.39 + 0.11 mT = 2.5 mT)

evaluated [28] yielding information at a time scale of ca. 100 ns. Photo-oxidation and NMR/CIDNP detection of reactive **1**-based intermediates was also reported. The CIDNP spectra were evaluated qualitatively [29, 30] and quantitatively [28, 31–33]. The corresponding data are presented in Table 1.

It is rather intriguing that there are fairly huge discrepancies between experimental data assigned to the 2c–3e radical cations. Here, the ^{14}N hfcs (hyperfine coupling constants) and the highest ^1H hfcs are most representative: Sevilla and coworkers report on a ^{14}N hfc of 3.3 mT whereas references [28, 32] reveal a value being two orders of magnitude smaller (0.01 mT). In the case of the ^1H hfc assigned to the proton in the α position, EPR and CIDNP data substantially deviate by the factor of 6 (0.14 vs. 0.87 mT). Generally, dominant hfcs of radicals rather markedly mirror their electronic (and steric) structure.

We have performed CIDNP experiments addressing the role of the oxidizing agent since it is known that the method of oxidation influences the reaction pathway and kinetics [5]. To assess the pH-dependent photo-reactivity of methionine, we have calculated the pK_a value of $\mathbf{1}^{\cdot+}$ in solution using state-of the art DFT calculations and QM/MM molecular dynamics calculations. Finally, we want to shed some light on the substantial inconsistence of the experimental hyperfine data assigned to the $\mathbf{1}^{\cdot+}$ based radicals. To this end, we present DFT calculated hfcs for the species presented in Scheme 1 because the experimental data have not been evaluated by comparison with their calculated counterparts although it has been well established that there are suitable DFT-based protocols for calculating almost matching hyperfine data for radicals like those shown in Scheme 1 [34–38].

2 Results and Discussion

2.1 ^{1}H CIDNP with Benzophenone-4-carboxylic Acid (B), Anthraquinone-1,5-disulfonic Acid Disodium Salt (AS) and 2-(Diphenylmethylene)malononitrile (CN)

CIDNP spectroscopy has been an efficient tool to follow reactions involving radical (ion) pairs [39–45]. This technique reveals the NMR fingerprint of products formed via radical reactions and the intensity pattern of polarized (non-Boltzmann populated magnetic states based on the formation of radical pairs) resonances provides an (indirect) information of intermediate radicals. This information is highly rewarding; however, the detected polarizations may stem from various reaction pathways and products. Such reactions may occur at time scales below ns, particularly, when they are based on monomolecular processes. Distinguishing between such overlapping effects even in geminate radical pairs may obstruct a clear-cut information derived from the CIDNP technique.

In many investigations, ketones and quinones serve as efficient oxidizing agents. Beside performing electron-transfer reactions, benzophenone-4-carboxylic acid (**B**) and the disodium salt of anthraquinone-1,5-disulfonic acid (**AS**) may also serve as hydrogen-abstracting agents in their excited states (or as electron/proton-transfer agents, but these two procedures are not distinguishable at the time scale of CIDNP). To be able distinguishing between hydrogen transfer and exclusively electron-transfer initiated reactions, we have additionally utilized 2-(diphenylmethylene)malononitrile (**CN**) as photo-reducing agent because the radical anion of **CN** does not serve as a proton acceptor (Scheme 2).

At pH 7.6, the use of **B** and **AS** yields polarized signals compatible with those already published [28–30, 32, 46]. For **B**, however, beside the polarized signals in the region of the resonances assigned to **1**, the broad emissive signal at 4 ppm points to the formation of (4-(hydroxy(phenyl)methyl)benzoic acid, the hydrated product of **B** in line with former observations [9]. With **AS**, a corresponding hydroquinone product cannot be established because its resonances overlap with those of the

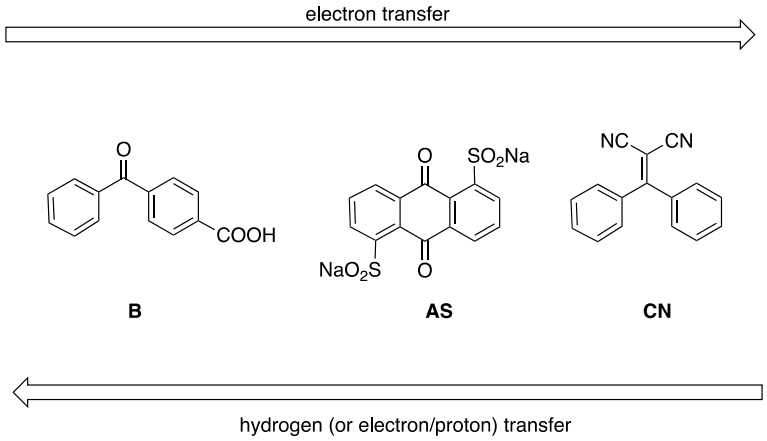

Scheme 2 Photo-reducing agents

parent quinone **AS** in the aromatic region. Markedly, excitation in the presence with 2-(diphenylmethylene)malononitrile (**CN**) does not yield any polarized (CIDNP) signals (Fig. 1, left, bottom).

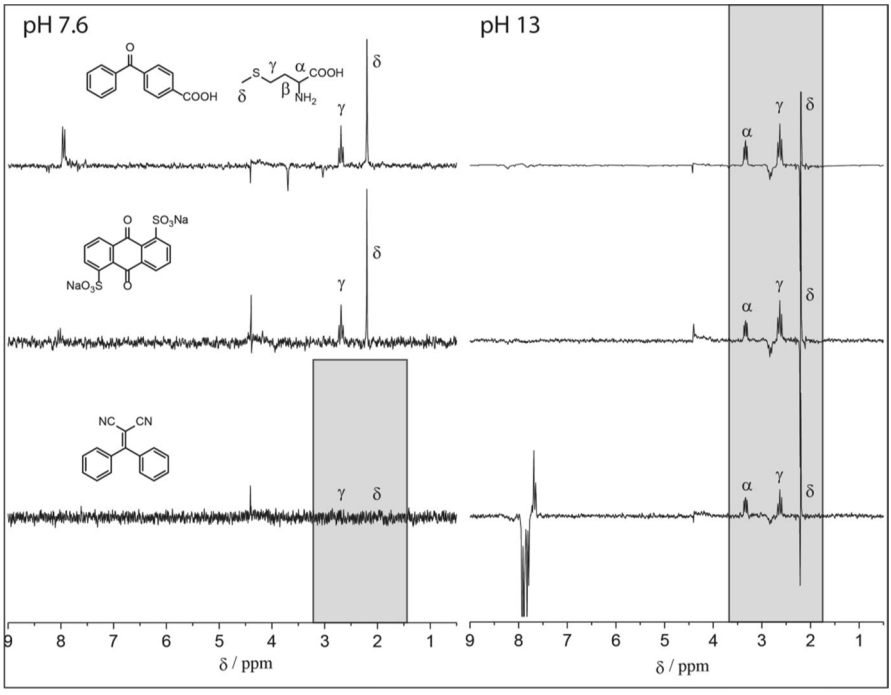

Fig. 1 ^{1}H-CIDNP spectra obtained upon photooxidation of **1** with **B** (top), **AS** (middle) and **CN** (bottom) a) at pH 7.6 and b) pH 13. All spectra are recorded 1 μs after the laser flash (355 nm, 8 ns and correspond to those shown in [33], 100 μs after the laser pulse)

Remarkably, under basic conditions, all three photooxidants yield compatible spectra/polarizations concerning the signals based on **1**, however, the intensity ratios between the resonances connected with the α, β, γ, and δ protons differ depending on the photooxidant. This reveals that **B**, **AS**, and **CN** may display different reactivities vs. **1**. The observation that no CIDNP effects are present, when **1** is irradiated in the presence of **CN** at pH 7.6 but the use of **B** and **AS** produces well distinguishable polarized signals indicates that (formal) hydrogen-atom transfer is very likely a decisive factor for the formation of CIDNP-detectable products. This assumption is additionally borne out by the fact that at higher pH (11–13, see Fig. 1, right, bottom and Supporting Information) even the use of **CN** leads to polarized NMR signals based on **1**. This emphasizes that the neutral radicals **D**• and **G**• (established by EPR [26]) could contribute to the polarizations in the CIDNP spectra. This assumption is substantiated our calculations, which indicate that the pK_a of $\mathbf{1}^{\bullet+}$ is *ca*. 10 (see next section). Moreover, the formation of **D**• and **G**• accounts for substantial polarizations of the protons in the β, g, and δ positions (see exp. and calc data in the Table 1) and only small ones for the α position. Another product, **K**, formed upon the well-established decarboxylation of $\mathbf{1}^{\bullet+}$ [26] likely leads to the polarized emissive triplet at ca 2.7 ppm assignable to its α protons of **K** (Fig. 1b) without significant changes in the polarization of the triplet of the α proton of **1** at 4 ppm.

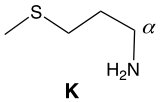

K

Consulting the calculated ^{1}H hfcs for the 2c–3e species $\mathbf{SN}^{\bullet+}$, a highly dominating polarization would be expected for the resonance of the α proton (^{1}H hfc of 2.88 mT, being 3 times higher than those of any other protons in $\mathbf{SN}^{\bullet+}$, see the Table 1 and Sect. 2.3). Accordingly, the dominating polarization should exist for the signal of the α proton at 3.6 ppm if $\mathbf{SN}^{\bullet+}$ is formed at a significant yield (in this context it is also important to note that the radicals centered at S or the adjacent atoms, **D**· and **G**·, possess basically identical hyperfine values independent on methionine being decarboxylated or not [26]).

2.2 Determination of the pK_a Value of $1^{\bullet+}$ by Theory

Recent computations involving explicit solvent molecules and molecular dynamics simulations indicate a rather subtle energy hypersurface upon the oxidation of **1** [2] with a rather shallow minimum for $\mathbf{SN}^{\bullet+}$. We have performed QM/MM molecular dynamics simulations and DFT calculations to get insight into the pK_a value of $\mathbf{1}^{\bullet+}$, particularly because the two well-established radicals **D**· and **G**· point to an efficient deprotonation of the primary radical $\mathbf{1}^{\bullet+}$. Using the thermodynamic cycle indicated in Scheme 3, we have calculated the energetics for the deprotonation of $\mathbf{1}^{\bullet+}$ to yield **G**·. Both, the DFT and the QM/MM procedure predict a rather high C, H acidity of $\mathbf{1}^{\bullet+}$ ($pK_a = 6.9$ and 7.8, respectively). These results point to an efficient reaction

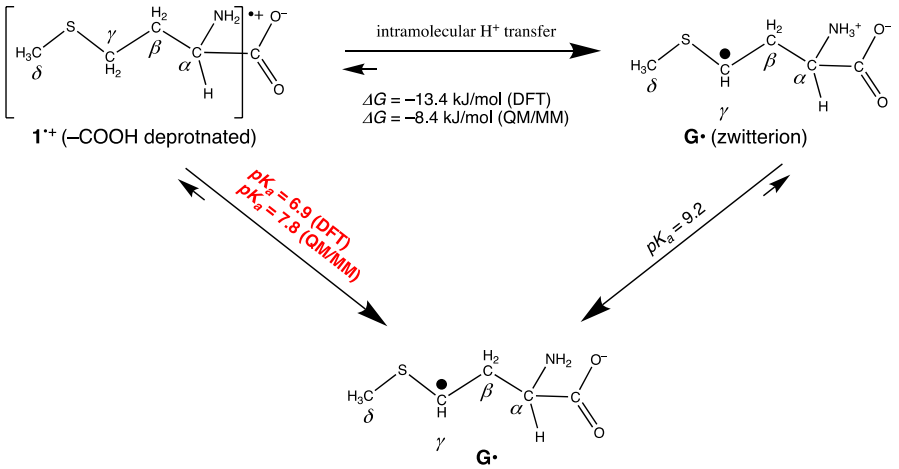

Scheme 3 Thermodynamic cycle for calculating the pK_a value for the deprotonation of $\mathbf{1}^{\cdot+}$ to yield $\mathbf{G}\cdot$

channel upon the oxidation of **1** at even slightly basic conditions to form neutral radical $\mathbf{G}\cdot$ (and, very likely, $\mathbf{D}\cdot$). Accordingly, beside decarboxylation, the formation of 2c–3e radical cations, and the aminyl radical $\mathbf{N}\cdot$, two additional reaction pathways of $\mathbf{1}^{\cdot+}$ must be considered.

DFT calculations and QM/MM simulations indicate that the (–COOH) deprotonated radical based on $\mathbf{1}^{\cdot+}$ has a global energy minimum for the 2-c 3-e conformation of the type $\mathbf{SN}^{\cdot+}$ (see also Scheme 4, below). Other conformations decarboxylate or undergo C–H or N–H deprotonation. In the case of the QM/MM simulations, the cleavage of C–COO bond can be seen on the lower picosecond time scale (5–50 ps). Thus, if one considers that the oxidation of deprotonated methionine occurs in a conformation without a preformed 2-c 3-e bond, we can assume that the decarboxylation strongly competes with the conformational relaxation.

2.3 Hyperfine Data, EPR Spectra and CIDNP Polarizations

The experimental investigations on the oxidation of methionine by electrochemical, chemical, photochemical, and pulse-radiolytic methodology spans over many decades. Paramagnetic-resonance methods, i.e., EPR, CIDEP (time-resolved EPR in the ns–μs time regime) and CIDNP have been particularly useful because they provide the steric and electronic structure of even short-lived radicals. Starting in the late 1980s, substantial progress has been made to calculate hyperfine data (predominately DFT) of various radicals and radical ions [34, 36–38, 47] (just for a few examples). Generally, the deviation between calculated and experimental hfcs hardly exceeds 10%. To fill the gap for the radicals presented and discussed above, we have calculated their hyperfine data. They are presented and compared with their experimental counterparts in Table 1. These ^{1}H- and ^{14}N hfcs do not only reflect the splittings established by EPR but they are also decisive for the CIDNP polarizations of the signals attributed to geminate radical pairs [48–50].

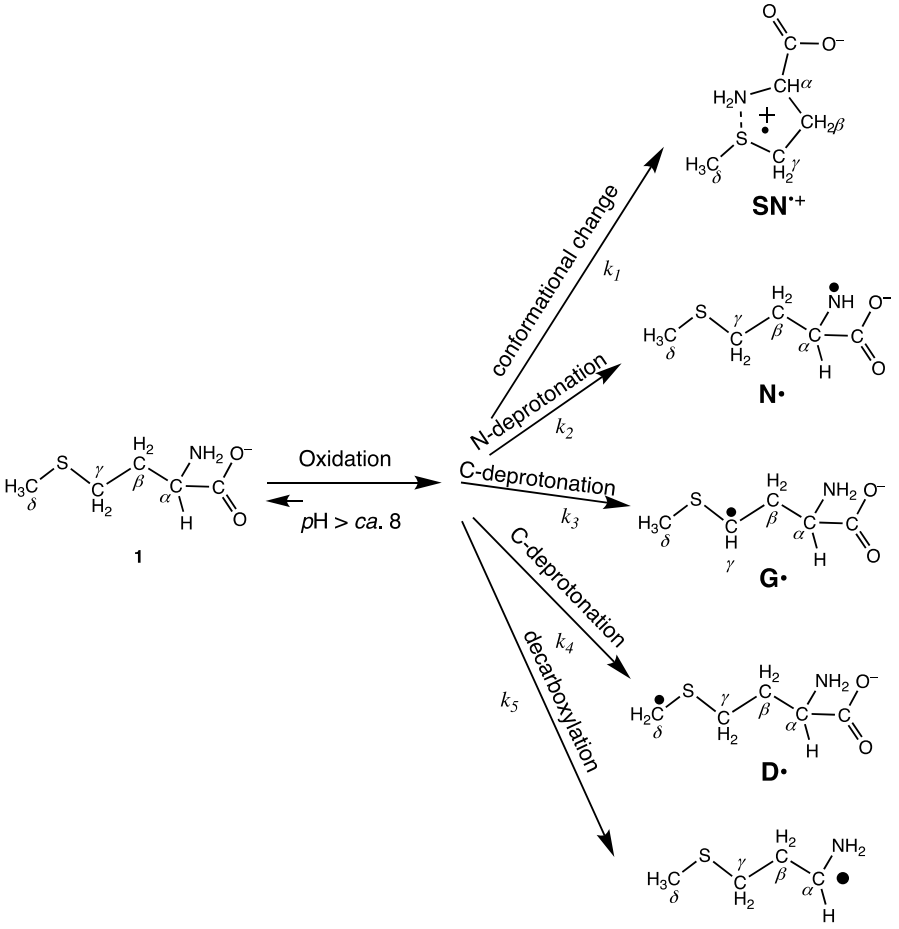

Scheme 4 Radicals involved in primary processes (ns–µs time scale) upon the oxidation of **1** under basic conditions (for better comparison the negative charges are omitted from the acronyms of the radicals)

For aminyl radical **N**·, the dominating ^{1}H hfc attributed to the two equivalent protons is predicted to be 2.2 mT, and the experimental counterpart is 2.19 mT; for the ^{14}N hfc these values are 1.46 and 1.34 mT, respectively. The same convincing agreement between experiment and prediction holds for radicals **D**· (e.g., calc: 1.73 mT, exp: 1.64 mT for the protons at the *d* position) and **G**· (e.g., calc: 1.93 mT, exp: 1.68 mT for the protons at the *g* position, Table 1).

For the 2c–3e configured **S**.·.**N**·$^{+}$ radical cation (in some cases referred as a neutral radical, when the acidic group of methionine is deprotonated, but that does not change the electronic character of the radical), Sevilla and coworkers have reported a dominating splitting of 3.3 mT (Table 1) upon irradiating **1** in a matrix at low temperature [24]; this value corresponds well to the dominant calculated values of 2.88 mT (^{1}H hfc, *a*-methyl group) and 2.42 mT (^{14}N hfc). Such prevailing ^{14}N hfcs

are characteristic for 2c–3e systems involving nitrogen centers because the s-orbital character at N rises (increasing the Fermi contact interaction) based on the formation of a new *s* bond formed by the N lone pairs [51–54]; the same holds for corresponding cationic sulfur radicals [55].

There is, however, a substantial contrast between the calculated hfcs and the experimental values presented in [28–32]. In [28] an experimental ^{14}N hfc of 0.01 mT and a ^{1}H hfc of 0.14 mT (*a*-methyl group EPR) have been reported. ^{1}H-CIDNP investigations also reveal small ^{1}H hfcs for the *a*-methyl group (0.87, 1.0 mT [31, 32]). All these latter values are significantly smaller than the DFT calculated predictions for the ^{14}N hfc (2.42 mT calc, deviation 2420%) and ^{1}H hfc (2.88 mT, deviation 300%) of the 2c–3e radical cation **SN**$^{\cdot+}$ indicating …

3 Conclusion

Our CIDNP upon oxidation of **1** with **B**, **AS**, and **CN** indicate that either the oxidizing agent must be able accepting protons or a pH above 10 is required to observe CIDNP polarizations. QM/MM and DFT calculations bear out that the primary methionine radical cation **1**$^{\cdot+}$ possesses C–H acidity and beside the aminyl radical **N**·, the C-centered radicals **D**· and **G**· are likely to be formed at a sub nanosecond time scale. Additionally, it is established that a sulfoxide is formed, and decarboxylation appears. Moreover, the 2c–3e radical (cation) **SN**$^{\cdot+}$ represents an energy minimum. This is a vast palette of reactions and is in harmony with the well-established electrochemical studies on **1** [3, 56] always indicating irreversible oxidations.

Exceeding deviations between the experimental (time-resolved-EPR (CIDEP) and CIDNP) hfcs for the 2c–3e radical (cation) **SN**$^{\cdot+}$ and the computed counterparts (Table 1) appeared.

Accordingly, we suggest that at the time scale of the detection of the CIDEP and CIDNP experiments, a subtle mixture of products is formed comprising radicals **N**·, **D**·, **G**·, **SN**$^{\cdot+}$, (Scheme 4) possibly **Al**$^{\cdot+}$ and closed-shell species like decarboxylation product **K**. Several of these radicals are likely components of the CIDEP spectra (at pH values above ca.7) and are also candidates for generating (geminate) CIDNP polarization because the deprotonation and the electron transfer are partially reversible and appear at ns to µs time scales (compatible rate constants k_1–k_5, Scheme 4). Product **K** is detectable via CIDNP as the result of an "escape" reaction. The overlay of the contributions of all these radicals to CIDNP polarizations makes the analysis of the corresponding spectra difficult.

It would be interesting developing a sound concept describing the follow-up reactions of methionine-based kinetic criteria. It should be also informative performing CIDNP with ^{13}C labeled isomers of **1**.

4 Experimental

All chemicals and deuterated solvents were purchased from Sigma-Aldrich and used without any additional treatment.

^{1}H NMR and CIDNP spectroscopic experiments were performed on a Bruker AVANCE 200 MHz DPX NMR spectrometer equipped with a wide bore ^{1}H-CIDNP probe. In TR-CIDNP experiments, composite pulse pre-saturation followed by a short (8 ns) 355 nm (90 mJ) laser flash and 2 µs (30°) radiofrequency pulse provided the observation of pure CIDNP polarizations. "Dummy" CIDNP spectra without the application of a laser pulse were always recorded to ensure an effective suppression of background NMR signals. All samples were bubbled for 5 min with nitrogen gas prior to experiments to remove oxygen from the reaction solution.

Quantel Brilliant B Nd/YAG laser operating on its third harmonic (355 nm) was used as an UV irradiation source.

The hyperfine coupling constants (hfc) of the free radicals were calculated using the Gaussian 09 package [57]. For the calculations of the pK_a value of deprotonated $\mathbf{SN}^{\cdot+}$ we tested two different procedures. The DFT procedure estimates the change in free energy for the H-transfer ($\mathbf{SN}^{\cdot+} \rightarrow$ zwitterionic $\mathbf{G}^{\cdot}$) with a conductor-like implicit solvation model [58] at the UB3LYP/6-311+G(2df,2p)//6-31G* level using conformational averaging. The free-energy change is −13.4 kJ/mol. To probe the explicit influence of the solvent and entropic contributions, we also used a procedure that is based on molecular dynamics (MD) simulations with a QM/MM-Hamiltonian: the radical species are described by self-consistent-charge DFTB [59, 60] (QM region) and the aqueous solution by 560 flexible water molecules [61] (MM region). The free-energy difference between deprotonated $\mathbf{SN}^{\cdot+}$ and zwitterionic $\mathbf{G}^{\cdot}$ is determined from MD-based umbrella sampling. The free-energy change is −8.4 kJ/mol.

Assuming a pK_a of 9.2 for the zwitterionic $\mathbf{G}^{\cdot}$ ($=pK_a$ of the NH_3-group of zwitterionic methionine in water), we can determine a free-energy difference of +53.1 kJ/mol for this deprotonation process at standard conditions (pH = 1). Using the thermodynamic cycle of Scheme 3, the standard free-energy change for the deprotonation of $\mathbf{SN}^{\cdot+}$ can be determined. It is +39.7 kJ/mol for the DFT approach and +44.7 kJ/mol for the QM/MM approach. These values translate into the pK_a values given in Scheme 3.

The conformational dynamics of deprotonated $\mathbf{SN}^{\cdot+}$ was studied by monitoring the axial and equatorial positions of the carboxy and methyl group during umbrella-sampled MD simulation at reaction coordinate of 0.8 (= local minimum that corresponds to deprotonated $\mathbf{SN}^{\cdot+}$).

Details of the DFT approach: we first performed a conformational search using the MMFP94-force field. Located conformations were then optimized at the UB3LYP/6-31G* level with the implicit solvation model C-PCM [58]. Localization of minima was verified by normal mode calculations. This led to 4 conformers for deprotonated $\mathbf{SN}^{\cdot+}$ and 16 conformers for zwitterionic radical $\mathbf{G}^{\cdot}$. The relative free energy between these two species were determined by Boltzmann-averaging of the UB3LYP/6-311+G(2df,2p) single-point energies of the 4/16 conformers. Including vibrational contributions from the normal mode calculations did not significantly alter the free-energy difference. Accordingly, the H-transfer (deprotonated $\mathbf{SN}^{\cdot+} \rightarrow$ zwitterionic $\mathbf{G}^{\cdot}$) relates to a free-energy change of −13.4 kJ/mol. All calculations were carried out with Spartan 20 [62].

Details of the QM/MM approach: third-order SCCDFTB was carried out with a damping exponent of 4.0 for H-interactions and the parameter set 3OB:nmod-1-2

with re-optimized parameters for N(sp3)–H interactions [63]. The potential of mean force for the H-transfer from deprotonated $\mathbf{SN}^{\cdot+}$ to zwitterionic $\mathbf{G}^{\cdot}$ was determined by umbrella sampling [64] using the relative position of the modified center of excess charge (Eq. 11 of Ref. [65]) as reaction coordinate. To define the excess charge, we used the heteroatoms C(γ) and N and the hydrogens connected to these atoms and the parameters rsw=1.15 and dsw=0.045. For the umbrella sampling, 19 MD simulations at equally spaced values of the reaction coordinate (from −0.9 to 0.9) were performed; the system was kept near the desired value of the reaction coordinate with a harmonic restraining potential and a force constant of 1600 kJ/mol. All covalent bonds (except those involving the transferred hydrogen) were very slightly restrained to avoid decarboxylation (see Sect. 2) or other undesired transformations during the unphysical H-transfer process. The average restraining energy is less than 0.1 kJ/mol at the end states of the H-transfer. The simulations were carried out at constant pressure (1 atm) and temperature (303.15 K) using Particle mesh Ewald summation for long range electrostatic interactions. The time step was 0.5 fs, and the length of each simulation was 500 ps. The first 100 ps served for equilibration and are not considered for the calculation of the PMF. All simulations were carried out with the program CHARMM (c43b2) using default settings for the aforementioned simulation model [66]. PMF profiles were calculated with Alan Grossfield's code of WHAM [67]. Accordingly, a free-energy change of -8.4 ∓ 1.0 kJ/mol relates to the H-transfer from deprotonated $\mathbf{SN}^{\cdot+}$ to zwitterionic $\mathbf{G}^{\cdot}$. Error bars correspond to the standard error of the mean when averaging over four blocks of data; each block contains 19 × 100 ps of simulation data. The pKa-value of $\mathbf{1}^{\cdot+}$ was calculated as follows: $pK_a(\mathbf{1}^{\cdot+}) = [2.3RT\ pK_a(Z) + \Delta G]/2.3RT$ where $pK_a(Z)$ is the pKa-value of zwitterionic methionine (=9.2) and ΔG is the free-energy change for the proton transfer (−13.4 kJ/mol with DFT or −8.4 kJ/mol with QM/MM).

Supplementary Information The online version contains supplementary material available at https://doi.org/10.1007/s00723-022-01469-9.

Acknowledgements We thank Daniel Rettenwander (TU Graz) for preliminary calculations of methionine-derived radicals and are indebted to Chrissostomos Chatgilialoglu (Bologna) for very fruitful discussions.

Funding Open access funding provided by Graz University of Technology. This study was supported by technische universität graz. MS is grateful to the Computer Center of the University of Strasbourg for computational resources (grant g2021a278c).

References

1. R.L. Levine, J. Moskovitz, E.R. Stadtman, IUBMB Life **50**, 301 (2000)
2. P. Archirel, C. Houee-Levin, J.L. Marignier, J. Phys. Chem. B **123**, 9087 (2019)
3. D. Kyriacou, Nature **211**, 519 (1966)
4. D. Scuderi, J. Bergès, P. de Oliveira, C. Houée-Levin, Radiat. Phys. Chem. **128**, 103 (2016)
5. M.J. Davies, Biochem. J. **473**, 805 (2016)
6. K. Bobrowski, C. Schoneich, J. Holcman, K.D. Asmus, J. Chem. Soc. Perkin Trans. **2**, 353 (1991)
7. M. Bonifacic, H. Mockel, D. Bahnemann, K.D. Asmus, J. Chem. Soc. Perkin Trans. **2**, 675 (1975)
8. K. Bobrowski, C. Houee-Levin, B. Marciniak, Chimia **62**, 728 (2008)
9. K. Bobrowski, G.L. Hug, B. Marciniak, H. Kozubek, J. Phys. Chem. **98**, 537 (1994)
10. K.O. Hiller, K.D. Asmus, Int. J. Radiat. Biol. **40**, 597 (1981)
11. G.L. Hug, K. Bobrowski, H. Kozubek, B. Marciniak, Photochem. Photobiol. **68**, 785 (1998)
12. T. Pedzinski, K. Bobrowski, B. Marciniak, P. Filipiak, Molecules **25**, 877 (2020)
13. K.D. Asmus, M. Gobl, K.O. Hiller, S. Mahling, J. Monig, J. Chem. Soc. Perkin Trans **2**, 641 (1985)
14. K.D. Asmus, M. Goebl, K.O. Hiller, S. Mahling, J. Moenig, J. Chem. Soc. Perkin Trans. **2**, 641 (1985)
15. K. Bobrowski, C. Schoeneich, J. Holcman, K.D. Asmus, J. Chem. Soc. Perkin Trans. **2**, 353 (1991)
16. K. Bobrowski, C. Schoneich, J. Holcman, K.D. Asmus, J. Chem. Soc. Perkin Trans. **2**, 975 (1991)
17. R.S. Glass, G.L. Hug, C. Schoneich, G.S. Wilson, L. Kuznetsova, T.-M. Lee, M. Ammam, E. Lorance, T. Nauser, G.S. Nichol, T. Yamamoto, J. Am. Chem. Soc. **131**, 13791 (2009)
18. J. Holcman, K. Bobrowski, C. Schoeneich, K.D. Asmus, Radiat. Phys. Chem. **37**, 473 (1991)
19. J. Moenig, M. Goebl, K.D. Asmus, J. Chem. Soc. Perkin Trans. **2**, 647 (1985)
20. H. Mohan, K.D. Asmus, J. Phys. Chem. **92**, 118 (1988)
21. C. Schoeneich, A. Aced, K.D. Asmus, J. Am. Chem. Soc. **115**, 11376 (1993)
22. C. Schoneich, Biochim. Biophys. Acta **1703**, 111 (2005)
23. C. Schoneich, Antioxid. Redox Signal **26**, 388 (2017)
24. M.H. Champagne, M.W. Mullins, A.O. Colson, M.D. Sevilla, J. Phys. Chem. **95**, 6487 (1991)
25. K. Kawatsura, K. Ozawa, S. Kominami, K. Akasaka, H. Hatano, Radiat. EIT **22**, 267 (1974)
26. M.J. Davies, B.C. Gilbert, R.O.C. Norman, J. Chem. Soc. Perkin Trans. **2**, 731 (1983)
27. B.C. Gilbert, J.P. Larkin, R.O.C. Norman, J. Chem. Soc. Perkin Trans **2**, 272 (1973)
28. H. Yashiro, R.C. White, A.V. Yurkovskaya, M.D.E. Forbes, J. Phys. Chem. A **109**, 5855 (2005)
29. M. Goez, J. Rozwadowski, J. Phys. Chem. A **102**, 7945 (1998)
30. M. Goez, J. Rozwadowski, B. Marciniak, Angew. Chem. Int. Ed. **37**, 628 (1998)
31. S.E. Korchak, K.L. Ivanov, A.V. Yurkovskaya, H.-M. Vieth, ARKIVOC **8**, 121 (2004)
32. O.B. Morozova, K.L. Ivanov, A.S. Kiryutin, R.Z. Sagdeev, T. Kochling, H.M. Vieth, A.V. Yurkovskaya, Phys. Chem. Chem. Phys. **13**, 6619 (2011)
33. O.B. Morozova, S.E. Korchak, R.Z. Sagdeev, A.V. Yurkovskaya, J. Phys. Chem. A **109**, 10459 (2005)
34. V. Barone, R. Improta, N. Rega, Acc. Chem. Res. **41**, 605 (2008)
35. C. Puzzarini, J. Bloino, N. Tasinato, V. Barone, Chem. Rev. **119**, 8131 (2019)
36. R. Batra, B. Giese, M. Spichty, G. Gescheidt, K.N. Houk, J. Phys. Chem. **100**, 18371 (1996)
37. J.W. Gauld, L.A. Eriksson, L. Radom, J. Phys. Chem. A **101**, 1352 (1997)
38. M. Kaupp, M. Buhl, V.G. Malkin, *Calculation of NMR and EPR Parameters: Theory and Applications* (Wiley-VCH, Weinheim, 2004)
39. J. Bargon, Helv. Chim. Acta **89**, 2082 (2006)
40. H. Fischer, J. Bargon, Acc. Chem. Res. **2**, 110 (1969)
41. M. Goez, *Photo-CIDNP spectroscopy*, in Annual Reports on NMR Spectroscopy (Elsevier, 2009).
42. P.J. Hore, R. Kaptein, ACS Symp. Ser. **191**, 285 (1982)
43. H.D. Roth, Top. Curr. Chem. **163**, 131 (1992)
44. H.R. Ward, Acc. Chem. Res. **5**, 18 (1972)
45. A. Yurkovskaya, O. Morozova, G. Gescheidt, Structures and reactivity of radicals followed by magnetic resonance, in *Encyclopedia of Radicals in Chemistry, Biology and Materials*. (Wiley, Chichester, 2012)
46. M. Goez, V. Zubarev, J. Phys. Chem. A **103**, 9605 (1999)
47. T. Giovannini, P. Lafiosca, B. Chandramouli, V. Barone, C. Cappelli, J. Chem. Phys. **150**, 124102 (2019)

48. M.D.E. Forbes, L.E. Jarocha, S. Sim, V.F. Tarasov, Time-resolved electron paramagnetic resonance spectroscopy: history, technique, and application to supramolecular and macromolecular chemistry, in *Advances in Physical Organic Chemistry*. (Elsevier, London, 2013)
49. R. Kaptein, Chem. Commun. (1971). https://doi.org/10.1039/C29710000732
50. L.T. Kuhn, J. Bargon, Exploiting nuclear spin polarization to investigate free radical reactions via in situ NMR, in *In Situ NMR Methods in Catalysis*. (Springer, Berlin, 2007)
51. R.W. Alder, A.G. Orpen, J.M. White, Chem. Commun. (1985). https://doi.org/10.1039/C39850000949
52. J.P. Dinnocenzo, T.E. Banach, J. Am. Chem. Soc. **110**, 971 (1988)
53. F. Gerson, G. Gescheidt, U. Buser, E. Vogel, J. Lex, M. Zehnder, A. Riesen, Angew. Chem. Int. Ed. **28**, 902 (1989)
54. F. Gerson, G. Gescheidt, J. Knobel, W.B. Martin, L. Neumann, E. Vogel, J. Am. Chem. Soc. **114**, 7107 (1992)
55. C.H. Hendon, D.R. Carbery, A. Walsh, Chem. Sci. **5**, 1390 (2014)
56. A. Sanchez Perez, F. Lucena Conde, J. Hernandez Mendez, J. Electroanal. Chem. Interfacial Electrochem. **74**, 339 (1976)
57. M.J. Frisch, G.W. Trucks, H.B. Schlegel, G.E. Scuseria, M.A. Robb, J.R. Cheeseman, G. Scalmani, V. Barone, G.A. Petersson, H. Nakatsuji, X. Li, M. Caricato, A. Marenich, J. Bloino, B.G. Janesko, R. Gomperts, B. Mennucci, H.P. Hratchian, J.V. Ortiz, A.F. Izmaylov, J.L. Sonnenberg, D. Williams-Young, F. Ding, F. Lipparini, F. Egidi, J. Goings, B. Peng, A. Petrone, T. Henderson, D. Ranasinghe, V.G. Zakrzewski, J. Gao, N. Rega, G. Zheng, W. Liang, M. Hada, M. Ehara, K. Toyota, R. Fukuda, J. Hasegawa, M. Ishida, T. Nakajima, Y. Honda, O. Kitao, H. Nakai, T. Vreven, K. Throssell, J.A. Montgomery, J.E.P. Jr., F. Ogliaro, M. Bearpark, J.J. Heyd, E. Brothers, K.N. Kudin, V.N. Staroverov, T. Keith, R. Kobayashi, J. Normand, K. Raghavachari, A. Rendell, J.C. Burant, S.S. Iyengar, J. Tomasi, M. Cossi, J.M. Millam, M. Klene, C. Adamo, R. Cammi, J.W. Ochterski, R.L. Martin, K. Morokuma, O. Farkas, J.B. Foresman, D. J. Fox, Gaussian 09, Revision A.02
58. T.N. Truong, E.V. Stefanovich, Chem. Phys. Lett. **240**, 253 (1995)
59. M. Elstner, D. Porezag, G. Jungnickel, J. Elsner, M. Haugk, T. Frauenheim, S. Suhai, G. Seifert, Phys. Rev. B **58**, 7260 (1998)
60. Q. Cui, M. Elstner, E. Kaxiras, T. Frauenheim, M. Karplus, J. Phys. Chem. B **105**, 569 (2001)
61. R. Fuentes-Azcatl, M.C. Barbosa, J. Mol. Liq. **303**, 112598 (2020)
62. Y. Shao, L.F. Molnar, Y. Jung, J. Kussmann, C. Ochsenfeld, S.T. Brown, A.T.B. Gilbert, L.V. Slipchenko, S.V. Levchenko, D.P. O'Neill, R.A. DiStasio Jr., R.C. Lochan, T. Wang, G.J.O. Beran, N.A. Besley, J.M. Herbert, C.Y. Lin, T.V. Voorhis, S.H. Chien, A. Sodt, R.P. Steele, V.A. Rassolov, P.E. Maslen, P.P. Korambath, R.D. Adamson, B. Austin, J. Baker, E.F.C. Byrd, H. Dachsel, R.J. Doerksen, A. Dreuw, B.D. Dunietz, A.D. Dutoi, T.R. Furlani, S.R. Gwaltney, A. Heyden, S. Hirata, C.-P. Hsu, G. Kedziora, R.Z. Khalliulin, P. Klunzinger, A.M. Lee, M.S. Lee, W. Liang, I. Lotan, N. Nair, B. Peters, E.I. Proynov, P.A. Pieniazek, Y.M. Rhee, J. Ritchie, E. Rosta, C.D. Sherrill, A.C. Simmonett, J.E. Subotnik, H.L.W. Iii, W. Zhang, A.T. Bell, A.K. Chakraborty, D.M. Chipman, F.J. Keil, A. Warshel, W.J. Hehre, H.F.S. Iii, J. Kong, A.I. Krylov, P.M.W. Gill, M. Head-Gordon, Phys. Chem. Chem. Phys. **8**, 3172 (2006)
63. M. Gaus, A. Goez, M. Elstner, J. Chem. Theor. Comput. **9**, 338 (2013)
64. G.M. Torrie, J.P. Valleau, J. Comput. Phys. **23**, 187 (1977)
65. P.H. König, N. Ghosh, M. Hoffmann, M. Elstner, E. Tajkhorshid, T. Frauenheim, Q. Cui, J. Phys. Chem. A **110**, 548 (2006)
66. B.R. Brooks, C.L. Brooks, A.D. Mackerell, L. Nilsson, R.J. Petrella, B. Roux, Y. Won, G. Archontis, C. Bartels, S. Boresch, A. Caflisch, L. Caves, Q. Cui, A.R. Dinner, M. Feig, S. Fischer, J. Gao, M. Hodoscek, W. Im, K. Kuczera, T. Lazaridis, J. Ma, V. Ovchinnikov, E. Paci, R.W. Pastor, C.B. Post, J.Z. Pu, M. Schaefer, B. Tidor, R.M. Venable, H.L. Woodcock, X. Wu, W. Yang, D.M. York, M. Karplus, J. Comput. Chem. **30**, 1545 (2009)
67. A. Grossfield, WHAM: the weighted histogram analysis method, version 2.0.9, http://membrane.urmc.rochester.edu/content/wham